

## Characterization of Porosity of Electrodes and Separators in Fuel Cell Industry

Akshaya Jena and Krishna Gupta  
Porous Materials Inc  
20 Dutch Mill Road, Ithaca, NY 14850

### Abstract

Pore size, pore structure, permeability, and surface area are some of the important characteristics that need to be measured for designing efficient electrodes and separators as well as evaluating their performance. For such measurements, we used the PMI Capillary Flow Porometer. The pores of the sample were filled with a wetting liquid and then pressurized air was applied on one side of the sample to remove the liquid from the pores and increase the flow rate of the gas. The flow rate through wet and dry samples, measured as a function of gas pressure, yielded the pertinent data. The data were highly reproducible and accurate. This technique of pore characterization has a number of advantages over other techniques.

### INTRODUCTION

Electrodes and battery separators are critical components of fuel cells and batteries. In many designs, the gaseous fuel passes through the porous electrodes and reacts with other components in the electrolyte at the surface of the electrode. The pore surface area controls the rate of reaction. The resistance to flow is governed by the pore size distribution of the electrode and the permeability of the electrode. The battery separator separates the electrodes. The pores of the separator provide sufficient permeability for liquid to flow, and the largest pore of the separator allows only selected components of the electrolyte to pass through. Therefore, the pore structure of battery separators and electrodes needs to be monitored for efficient design and operation of these components. In this investigation, we used a capillary flow porometer to measure the largest pore size, pore size distribution, permeability, and surface area of electrode and separator materials.

### EXPERIMENTAL PROCEDURE

In this technique a sample of the material is soaked in a liquid that fills the pores in the sample spontaneously. The sample is loaded in the sample chamber (Figure 1) and is maintained at the desired temperature. Pressure of air or some other suitable gas on one side of the sample is gradually increased. The chamber is designed so that the gas passes either parallel to the thickness of the sample (Through-plane flow) or parallel to the plane of the sample (In-plane flow). The in-plane and the through-plane pore characteristics are separately determined by using the appropriate sample chamber.

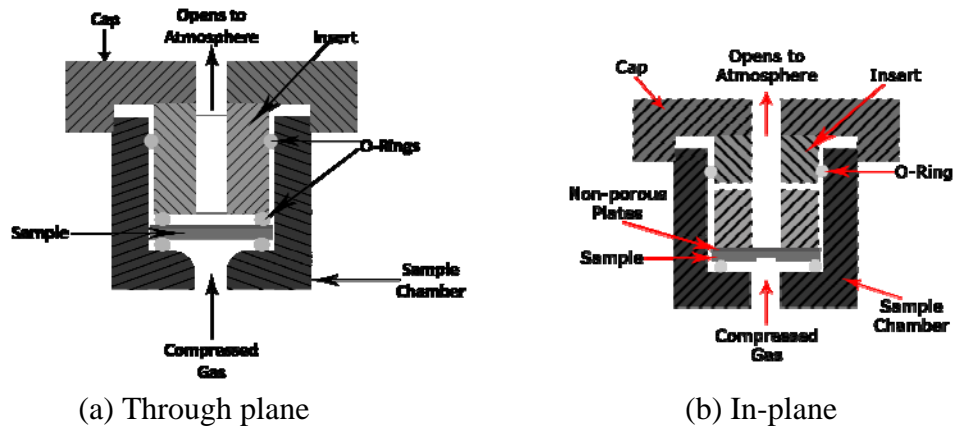


Figure 1. Sample chamber

Initially the gas does not flow through the sample because the liquid in the pores prevents flow. When the pressure is sufficient, liquid from the largest pore is emptied and the flow of the gas starts. With increase in pressure, smaller pores are emptied and the flow of gas increases. The PMI Capillary Flow Porometer was used in this study. It measured pressure and flow rate accurately. The data acquisition and management were carried out through windows based software [1,2]. The porometer generated highly reproducible data [3]. The pressure of gas and the corresponding flow rate were accurately measured using wet as well as dry samples. From these data, the largest pore size, pore size distribution, permeability, and surface area were calculated. A typical plot of flow rate as a function of pressure is shown in Figure 2.

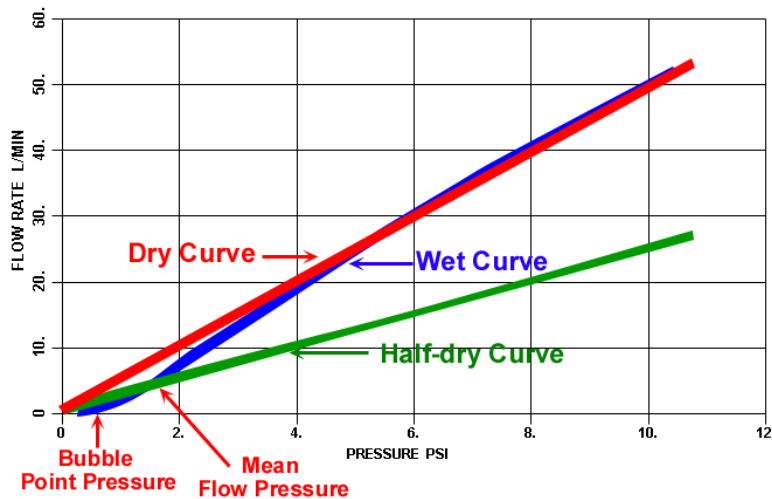


Figure 2. Variation of flow rate with differential pressure for battery separator #1.

## ANALYSIS

Filling the pores of a sample with a liquid involves creation of solid/liquid interfaces in place of solid/gas interfaces. If the solid/gas interfacial free energy is higher than the solid/liquid interfacial free energy, the process of filling the pores with liquid will decrease the free energy of the system and thus,

make the process spontaneous. The liquid that fills the pores spontaneously is known as a wetting liquid. When gas displaces liquid inside pores, the solid/gas interface replaces the solid/liquid interface, and the free energy of the system increases (Figure 3).

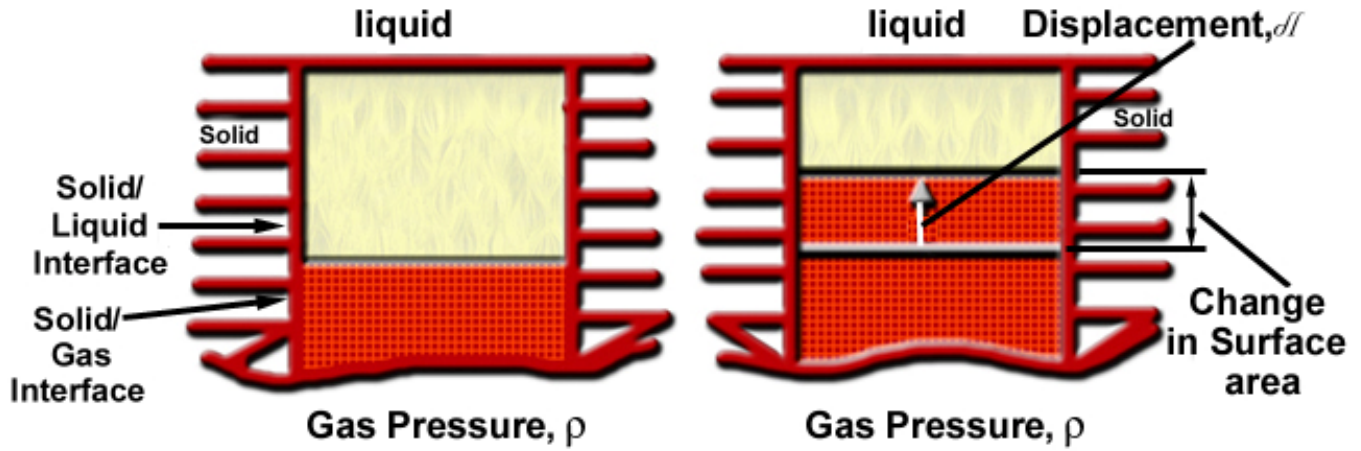


Figure 3. Displacement of liquid by gas.

In order to displace the liquid inside the pore, the gas does work on the system to compensate for the increase in the interfacial free energy [4]. The work done by the gas is represented by  $p dV$ , where  $p$  is the gas pressure at the inlet relative to that at the outlet and  $dV$  is the infinitesimal increase in volume of the gas inside the pore. The work done by the gas must be equal to the increase in the interfacial free energy. The displacement of the gas inside an opening changes the surface areas (Figure 4).

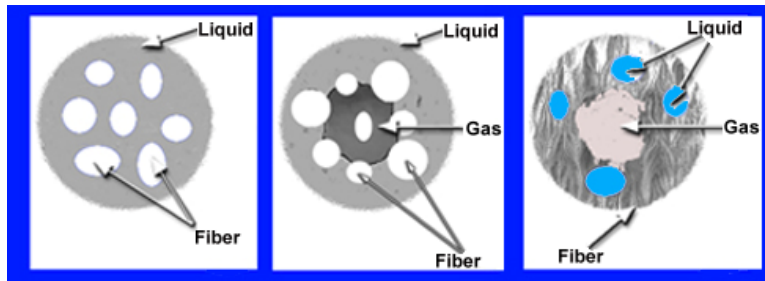


Figure 4. Increase in surface area. (a) Fibrous material containing liquid. (b) Opening in fibrous material filled with gas. (c) Opening in non-fibrous material filled with gas.

Let the increases in the solid/gas and liquid/gas surface areas due to infinitesimal increase in the volume of the gas, be  $dS_{s/g}$  and  $dS_{l/g}$  respectively. Then [5]:

$$p dV = (\gamma_{s/g} - \gamma_{s/l}) dS_{s/g} + \gamma_{l/g} dS_{l/g} \tag{1}$$

where:

- $\gamma_{l/g}$  = liquid/gas interfacial free energy
- $\gamma_{s/g}$  = solid/gas interfacial free energy
- $\gamma_{s/l}$  = solid/liquid interfacial free energy.

Equation 1 may be written as:

$$p = \gamma_{l/g} \beta (dS_{s/g} / dV) [ 1 + (f / \beta)] \quad (2)$$

where,  $\beta = [(\gamma_{s/g} - \gamma_{s/l}) / \gamma_{l/g}]$ , and  $f = (dS_{l/g} / dS_{s/g})$ .

Consideration of equilibrium between the three interfacial free energies (Figure 5) shows [6] that  $\cos \theta = (\gamma_{s/g} - \gamma_{s/l}) / \gamma_{l/g}$ , where  $\theta$  is the contact angle, and  $\beta = \cos \theta$ . For wetting liquids, normally  $\beta \sim 1$ . However, if the interfacial free energies are such that equilibrium is not possible (Figure 4), then  $\beta$  is greater than 1 [3].

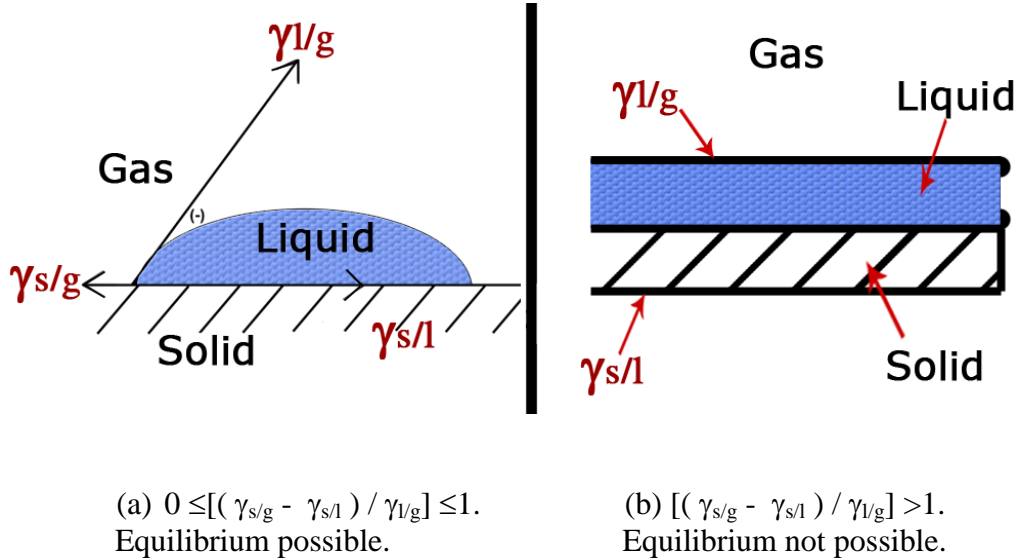


Figure 5. Equilibrium between surface tensions

It has been shown that  $\beta$  in Equation 2 is equal to 1 for wetting liquids with small values of interfacial free energy [3]. The magnitude of  $f$  in Equation 2 is determined by the structure of the path of gas flow. Paths are created by interconnected voids present in the filter. Normally, samples are either fibrous or non-fibrous. Cross-sections of typical paths in fibrous and non-fibrous materials are illustrated in Figure 4. The interfacial area of fibrous materials is almost entirely due to the outer surfaces of fibers, and the magnitude of the term  $(dS_{l/g} / dS_{s/g})$  is negligible. In case of non-fibrous materials, the term  $(dS_{l/g} / dS_{s/g})$  is zero. Consequently, for both non-fibrous and fibrous materials, Equation 2 reduces to:

$$p = \gamma_{l/g} \cos \theta (dS_{s/g} / dV) \quad (3)$$

The magnitude of  $(dS_{s/g} / dV)$  in this equation is a function of the location along the path of the gas. For a displacement  $dl$ , of the gas/liquid interface (Figure 3) at a location in a pore of circular cross-section of radius,  $r$ ,  $(dS/dV) = (2 \pi r dl / \pi r^2 dl) = (2/r)$ . This example illustrates the fact that  $(dS/dV)$  increases with decrease in the size of cross-section along the length of the pore. Because the pore size changes along the length of a pore, the pressure required to displace the liquid in the pore is different at different locations and has the maximum value at the pore's most constricted location. Therefore, the pressure required to clear a pore of the wetting liquid is determined by the maximum value of  $(dS/dV)$  at the most

constricted part of the pore. Thus, pressure is a measure of the size of the pore at its most constricted location. The arrows in Figure 6 illustrate the locations of the most constricted part of each pore.

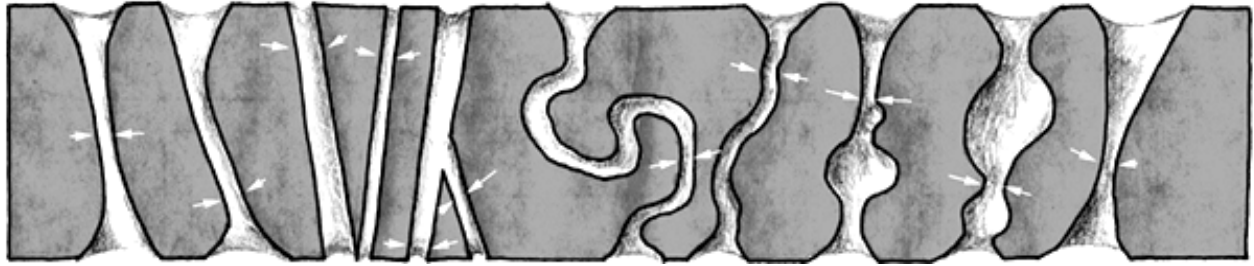


Figure 6. Sketch illustrating a range of pore sizes and the most constricted pore sizes

Equation 3 shows that pressure is a measure of  $(dS_{s/g}/dV)$  of the pore at its most constricted part. However,  $(dS_{s/g}/dV)$  is not a convenient quantity to use as the measure of pore size. For a circular cross-section of diameter  $D$ :

$$(dS_{s/g}/dV) = 4/D \tag{4}$$

However, in case of non-circular cross-sections (Figure 7),  $(dS_{s/g}/dV)$  cannot be specified in any simple way.

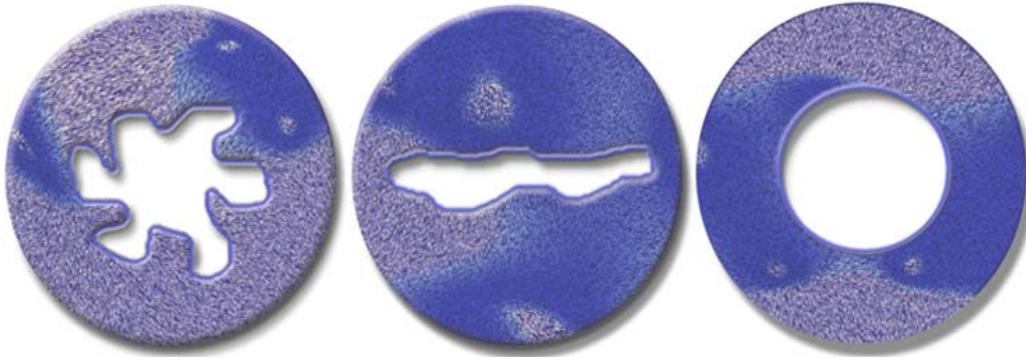


Figure 7. Examples of pore cross-sections

We define the diameter of a non-circular cross-section as the diameter of a circular opening that has a  $(dS_{s/g}/dV)$  value the same as that of the pore cross-section. Pore diameters defined in this manner are calculated using the following relation derived from Equations 3 and 4:

$$D = 4 \gamma_{l/g} \cos \theta / p \tag{5}$$

Thus, if  $p$  is the measured value of pressure that is required to empty a pore,  $D$  calculated from Equation 5 gives the diameter of an opening of circular cross-section whose  $(dS_{s/g}/dV)$  value is the same as that of the actual pore at its most constricted point.

## RESULTS AND DISCUSSION

### Pore diameter

The data obtained from the porometer (Figure 2) can be used to calculate a number of characteristics of the pore structure of the sample. The pressure at which the flow of the gas begins (The bubble point pressure), corresponds to the pressure required to empty the largest pore. This pressure is used to calculate the diameter of the largest pore in the sample. The half-dry curve in the figure gives half of the flow rate through the dry sample at the same pressure. The intersection of the wet and the half-dry curves give the mean flow pressure, which is used to calculate the mean flow pore diameter. The mean flow pore diameter tells us that half of the flow through a dry sample is through pores having diameter greater than the mean flow pore diameter. The largest pore diameter and the mean flow pore diameters of two battery separators and an electrode are listed in Table 1.

Table 1. Largest pore diameter and mean flow diameter

Sample	Largest diameter, $\mu\text{m}$	Mean flow diameter, $\mu\text{m}$
Battery separator		
#1	25.52	6.63
#2	36.73	26.60
Electrode	46.68	14.12

### Flow distribution

We use a model of the porous material in which the sample thickness is  $l$ , the pores are cylindrical of length  $l$ , and the pore diameter is proportional to the measured constricted

pore diameter. Assuming the flow to be viscous [7], and expressing the flow rate  $F$ , in volume at STP per unit time, we express the flow rate through the porous sample in the following form:

$$F = [\pi\beta / (128 \mu l 2p_s)] [p_i + p_o] [\sum_i N_i D_i^4] [p_i - p_o] \quad (6)$$

where,  $\mu$  is the viscosity of gas,  $p_s$  is the standard pressure,  $p_i$  is the inlet pressure,  $p_o$  is the outlet pressure,  $N_i$  is the number of pores of diameter  $D_i$ . The equation shows that the variables are separable and the flow rate may be expressed as the product of two functions;  $f(p)$  and  $g(D, N, \dots)$ . Thus:

$$F = f(p).g(D, N, \dots) \quad (7)$$

The ratio of  $F_{w,i}$  and  $F_{d,i}$ , which are the flow rates of wet and dry samples respectively at the same pressure  $p_j$ , becomes:

$$(F_{w,j} / F_{d,j}) = [g(D, N, \dots)]_{w,j} / [g(D, N, \dots)]_{d,j} \quad (8)$$

Thus,  $(F_{w,j} / F_{d,j})$  is independent of pressure at which it is measured. We define  $F(D)$  as the flow distribution function. Hence:

$$(F_{w,j} / F_{d,j}) = \int^{D_j} F(D)dD \tag{9}$$

$$F(D) = - d(F_{w,j} / F_{d,j}) / dD \\ = - [(F_{w,j+1}/F_{d,j+1}) - (F_{w,j}/F_{d,j})] / [D_{j+1} - D_j] \tag{10}$$

The fact that the flow rate increases with decrease in pore diameter, is incorporated in Equation10 by including the negative sign in the equation. The flow distributions, calculated for the battery separator and the electrode are presented in Figures 8 and 9.

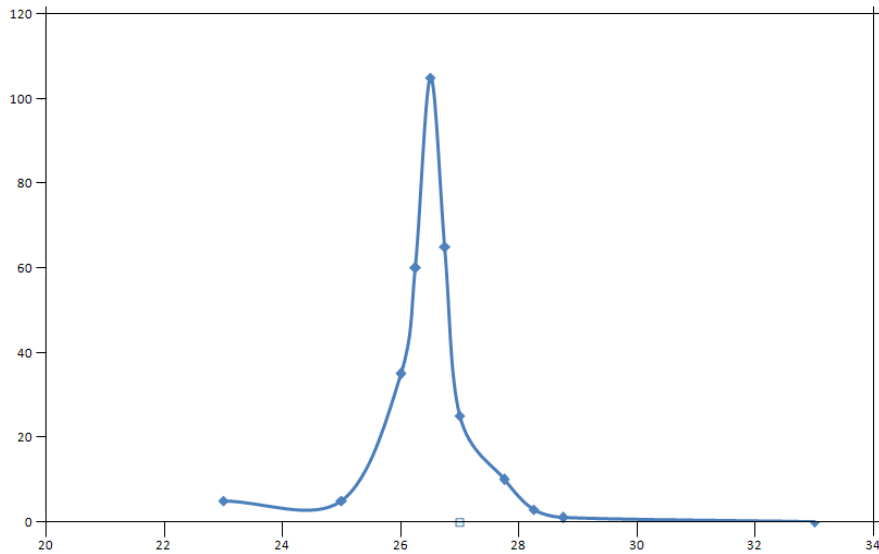


Figure 8 Flow distribution of battery separator #2.

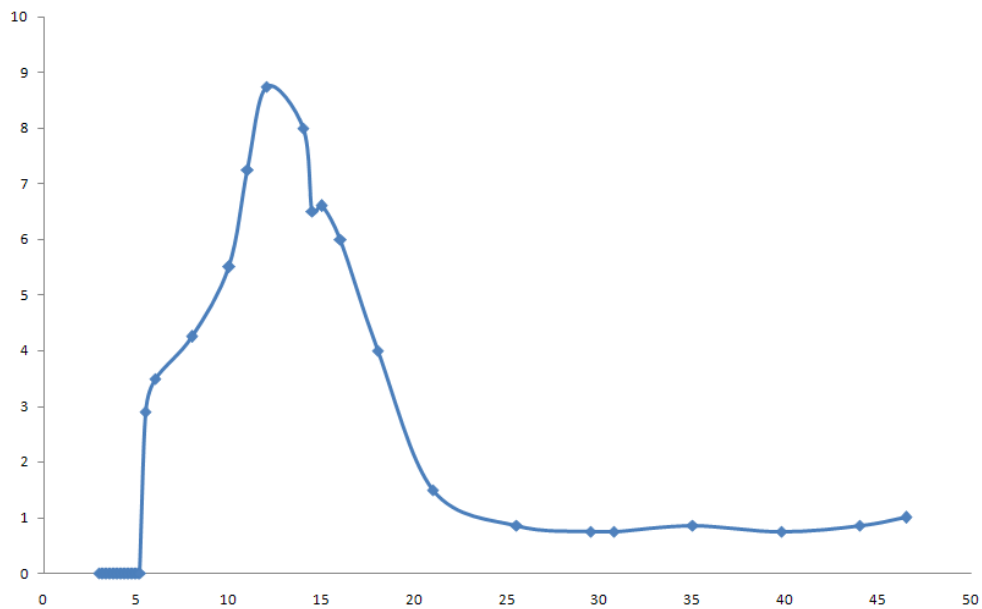


Figure 9. Flow distribution of Electrode.

## Permeability

Gas permeability  $k$ , through a sample is related to the flow rate through the following relation:

$$F = k (A / 2\mu l p_s) (p_i + p_o) [p_i - p_o] \quad (11)$$

where  $A$  is the surface area of the sample. Therefore, gas permeability is directly obtained from the dry curve. Permeabilities of the electrode and the battery separator #1, calculated from the dry curves are listed in Table 2 for three differential pressures.

Table 2 Air permeability of electrode and battery separator.

Differential pressure psi	Permeability of battery separator #1, $\times 10^3$ Darcy	Permeability of electrode, $\times 10^3$ Darcy
0.535	8.412	800.4
1.13	7.852	784.6
3.33	7.367	732.1

It is clear from the table that permeability depends upon the average pressure at which the measurement is made. The effect of pressure could be appreciable depending upon pore diameter, porosity, and tortuosity.

Liquid permeability of electrodes and battery separators can also be determined in the same instrument by measuring the liquid flow rate.

## Envelope surface area

The envelope surface area  $S$ , of all the through pores per unit weight of the sample of porosity  $P$ , and true density  $\rho$ , is given by:

$$S = [P/(1-P)\rho] \sqrt{[P(p_i - p_o) / (f l \mu v)]} \quad (12)$$

where  $v$  is the approach velocity and  $f$  is a constant that has a value of 5 for most materials. Porometer measures the approach velocity. The envelope surface area is calculated by combining the approach velocity measured in the porometer with values of porosity and true density measured separately by pycnometry.

## Advantages of capillary flow porometry

Flow porometry has a number of advantages over other techniques such as porosimetry and nitrogen adsorption.

- (1) No toxic material is used in the test.
- (2) Very high pressures, where the sample may get damaged or the pore structure may get distorted, are not used for the test.

- (3) The test is normally performed at room temperature rather than the liquid nitrogen temperature
- (4) The test is non-destructive. The sample is not damaged or contaminated. It is reusable.
- (5) The test does not require much preparation time and takes only a few minutes to be executed. This results in the saving of a lot of the operator's valuable time.
- (6) The fully automated instrument interfaces with windows based software for data acquisition and management. Thus, highly reproducible and objective data are obtained.
- (7) Only the through pores are tested. Therefore, this technique is more appropriate for characterizing battery separators and electrodes.

## CONCLUSIONS

1. Flow rates of air through wet and dry samples of an electrode and two battery separators were measured in the PMI Capillary Flow Porometer.
2. Using these data it was possible to calculate the largest pore size, the mean flow pore size, the distribution function of fractional flow for pores of various sizes, and permeability. It was also shown that the surface area of pores can be calculated if the porosity and the true density are measured separately using pycnometry.
3. The results were highly reproducible.
4. The technique of flow porometry that was used in this investigation has a number advantages over other techniques. Flow porometry does not use high pressures or very low temperatures. No toxic mater is involved in the test. The actual test takes only a few minutes and saves a lot of the operator's time.

## REFERENCES

1. R.V. Webber, Recent Advances in Automated High Accuracy Bubble Point Measurement, Filtration News, January/February, pp.52, 1994.
2. C.R. Stillwell, Recent Advances in Porometry and Porosimetry: Introducing the Microflow Porometer and the Aquapore Porosimeter, Proceedings of the 7<sup>th</sup>. World Filtration Congress, Budapest. Hungary, 1996.
3. Vibhor Gupta and A.K. Jena, Substitution of Alcohol in Porometers for Bubble Point Determination, Advances in Filtration and Separation Technology, Volume 13b, pp.833-44, American Filtration and Separation Society, 1999.
4. K. Denbigh, The Principles of Chemical Equilibrium, Cambridge University Press, London, 1968.
5. Akshaya Jena and Krishna Gupta, In-plane Compression Porometry of Battery Separators, Power Source 17, Ed. A. Attewell, Elsevier, PP.46, 1999.
6. A.W. Adamson, Physical Chemistry of Surfaces, Inter Science, New York, 1967.
7. A. E. Scheidegger, The Physics of Flow through Porous Media, Macmillan, New York, 1957.